

Electro-rheological Description of Solids Dielectrics Exhibiting Electrostriction

R. R. Mocellini, O. A. Lambri¹, F. G. Bonifacich², D. Gargicevich², F. Tarditti²

Laboratorio de Materiales (LEIM), Escuela de Ingeniería Eléctrica, Centro de Tecnología e Investigación Eléctrica (CETIE),
Facultad de Ciencias Exactas, Ingeniería y Agrimensura, Universidad Nacional de Rosario,
Av. Pellegrini 250, 2000, Rosario, Argentina

¹Member of the CONICET's Research Staff

²CONICET's fellowship

M. Anhalt³, B. Weidenfeller

Institute of Particle Technology, Clausthal University of Technology, D-38678 Clausthal-Zellerfeld, Germany

³Present address: FRÖTEK-Kunststofftechnik GmbH, An der Unteren Söse 24 – 30, D-37520 Osterode

and **W. Riehemann**

Institute of Materials Science and Engineering,
Clausthal University of Technology, D-38678 Clausthal-Zellerfeld, Germany

ABSTRACT

An electro-rheological model based in Voigt units which takes into consideration the variation in volume promoted by electrostriction is developed. The model was based on a mean field approximation as an averaging of the mechanical and electrical properties. The electro-rheological coupling which describes the effects of the electrical excitation on the mechanical response and the effects of the mechanical excitation on the electrical response of the dielectric is studied.

In the case of an alternating electrical excitation the model reveals the appearance of harmonics in the current through the dielectric promoted by the electrostriction phenomenon. In contrast, for the case of an oscillating mechanical excitation, a current which overtakes the driving mechanical oscillation was resolved to appear.

The correlation of the new model with experimental results, obtained from dynamic mechanical analysis tests conducted under high electric field, in polyamide, was found out.

Index Terms - Electro-rheology, engineering modeling, dielectric materials, electrostriction, DMA.

1 INTRODUCTION

THE relation between the strain and the square of the electric field strength in a dielectric material is called electrostriction [1, 2]. From an appropriate reciprocity relation, it follows that the application of a mechanical stress may produce a change in the dielectric properties [1, 3]. In a recent work, the electrostriction effect was studied by means of the theory of inclusions. The internal stresses promoted by the electrostriction phenomenon were monitored by studying the behavior of the misfit coefficient and the transfer of elastic energy process [4-6]. In fact, the model in [4] considers that applying an electric field to a dielectric

material leads to the stretching of dipoles giving rise to the appearance of inclusions. They promote the development of internal stresses in the dielectric material; whose electromechanical equilibrium condition was determined from the inclusion formalism [5, 6].

A general and formal treatment of the coupling of the mechanical and electrical properties in materials can be done by resolving the stress state from a general thermodynamic potential equation involving both contributions [1, 3, 4]. However, the mathematical handling of the resulting equations applied to engineering calculations in technological materials is always complicated.

Electro-rheological studies facilitate predictive analysis in the field of engineering of materials under coupled mechanical

and electrical stresses [7, 8]. A detailed electro-rheological model of the electrical and mechanical response of dielectric materials was reported in [7]. The model is based on a Voigt-type rheological representation either with two or three parameters. The model allows the description of the viscoelastic response of a dielectric material when it is subjected to an electrical excitation. It should be mentioned that for the model developed in [7], the volume of the dipole element was considered as a constant. In addition, the study was developed only by considering the effect of a variable electrical field applied to the dielectric material. Regarding the work in [8], the study was developed for two-phase dielectric materials with the aim of obtaining the dielectric response in frequency from dynamic mechanical analysis measurements. In addition, the work was carried out considering a constant volume of the dipole element.

In the present work, an electro-rheological model based on Voigt units which takes into consideration the variation in volume promoted by electrostriction is developed. The electro-rheological coupling which describes the effects of the electrical excitation on the mechanical response and the effects of the mechanical excitation on the electrical response of the dielectric is studied. The model is able to predict both, the appearance of harmonics in dielectric materials excited by an alternating electric field and the appearance of an alternating current in a dielectric material subjected to an oscillating mechanical field. In addition, the model was experimentally verified by means of dynamic mechanical analysis (DMA) measurements conducted under high electric fields.

2 THEORETICAL BACKGROUND

2.1 CONTINUOUS ELECTRODYNAMICS

Figure 1 shows a flow diagram of the interrelation between electrical and mechanical excitations and their responses. In technological applications it is often of interest the modelling of the energy flows from the electrical excitation (W_c) and the mechanical excitation (W_s) to the electrical response (W_a) and the mechanical response (W_m), including the electro-mechanical coupling.

Following the nomenclature used in Figure 1, the energy of the electric field can be written as [3],

$$W_c = \frac{1}{2} \iiint_V \mathbf{D} \cdot \mathbf{E} \, dv \tag{1}$$

where \mathbf{D} and \mathbf{E} are the displacement and electric field vectors, respectively, satisfying the condition,

$$\mathbf{D} = \epsilon_0 \mathbf{E} + \mathbf{P} \tag{2}$$

In equation (2) \mathbf{P} is the polarization vector and ϵ_0 the vacuum permittivity. For one-dimensional geometry, i.e. plane parallel plates, equation (1) can be written as,

$$W_c = \frac{1}{2} A \int_0^d D E \, dx \tag{3}$$

where d is the gap between the plates and A is the area of each plate. Considering that the material is isotropic, equation (3) may be written as,

$$W_c = \frac{1}{2} A \int_0^d (\epsilon_0 E + P) E \, dx \tag{4}$$

or as,

$$W_c = \frac{1}{2} A \int_0^d \epsilon_0 E^2 \, dx + \frac{1}{2} A \int_0^d E P \, dx \tag{5}$$

Corresponding to the schematic representation given in Figure 1, W_c satisfy the following condition of thermodynamic equilibrium,

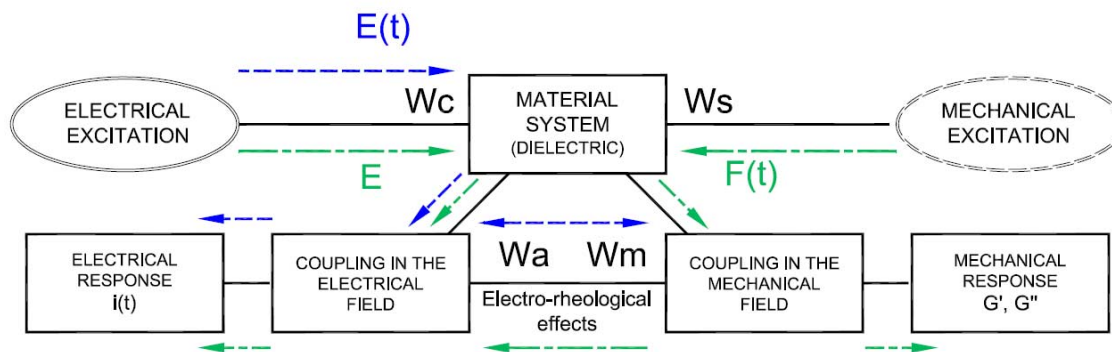


Figure 1. Flow diagram of the interrelation between electrical and mechanical excitations and responses. Dashed arrows indicate the flow for an electrical excitation. Alt-dashed arrows indicate the flow for a mechanical excitation under constant electric field. See explanation in the text. Adapted from [7].

$$W_C = W_a + W_m \quad (6)$$

The induced polarization charge, $\sigma_i = q_i / A$, in the interface of a dielectric material, which is exposed to a constant electric field, E_o , can be calculated from the Gauss theorem, as it was already shown in [7],

$$\sigma_i = E_o \varepsilon_o \left(1 - \frac{1}{\varepsilon_r} \right) \quad (7)$$

The stress p_x acting at a surface A in a dielectric material of constant ε_r , which is displaced by a distance x , due to the polarization produced by an electric field between the plates separated by a gap, d , can be written as follows [9-11],

$$p_x = \frac{F_x}{A} = \frac{1}{2} \varepsilon_o E_o^2 \left(1 - \frac{1}{\varepsilon_r} \right) \quad (8)$$

where F_x is the corresponding force.

Combining equations (7) and (8) we can write,

$$p_x = \frac{1}{2} \sigma_i E_o \quad (9)$$

The surface polarization charge density is represented by the projection of the polarization vector over the surface of the dielectric, and therefore equation (5) can be written as,

$$W_C = \frac{\varepsilon_o A}{2} \int_o^d E^2 dx + \frac{A}{2} \int_o^d E \frac{q_i}{A} dx \quad (10)$$

It must be mentioned that in the second integral in equation (10), the induced charge q_i resides on the surface of the dielectric. Considering a constant electric field in the dielectric is between the two parallel plates, the first integral results in,

$$W_a = \frac{\varepsilon_o A}{2} E^2 d \quad (11)$$

while the second one can be written as,

$$W_m = \frac{1}{\varepsilon_r} \int F_x dx \quad (12)$$

Consequently, the energy transferred to the dielectric material is

$$W_C = \frac{1}{2} \varepsilon_o E^2 V + \frac{1}{\varepsilon_r} \int F_x dx \quad (13)$$

This expression represents the energy transfer to an electro-mechanical system.

2.2 ELECTRO-RHEOLOGICAL DESCRIPTION

We have described in previous works the dielectric material as an assembly of discrete dipoles and inter-dipole elements linked between them [7, 8]. A dipole together with an inter-dipole element was defined as the so called elementary unit [7]. Dipoles and inter-dipoles were described by means of Voigt rheological models either with two or three parameters. In the case of two parameter Voigt units, the dipole is composed by: (a) a capacitor of plane charged plates which promote the separation of the plates under the application of the electric field E , (b) a spring, k_D , which represents the elastic constraints of the matrix and (c) a dashpot, b_D which represents the energy loss by irreversibility, see Figure 2. The inter-dipole element is composed by a spring k_{id} and a dashpot b_{id} .

In addition, a two dimensional representation of a dielectric material was made considering a dielectric solid material having an internal structural arrangement which allows the orientation of dipoles by applying an external electric field [7]. It is assumed that the randomly oriented dipoles already exist in the dielectric material matrix, giving rise to a null polarization vector, Figure 3. The dipole itself, during the rotation, was assumed to not change its length, i. e. it is under pure rotation. This rotation promotes on the inter-dipole space, through a mean field approximation, compression and tensile effects as shown in Figure 3 [7].

3 EXPERIMENTAL

3.1 SAMPLES

As matrix materials a polyethylene (PE) grade Moplen EP F 31 H (Basell B.V., Klundert, The Netherlands) and polyamide (PA) grade Ultramid B3 (BASF, Mannheim, Germany) with crystalline melting temperatures of $T_M = 350$ K and 493 K, respectively; were chosen. Polymer samples were prepared from pellets, using an injection moulding machine (Allrounder 320C 600-250, Arburg, Germany). Samples of parallelepiped form of 10 mm width, 1.4 mm thick and 48 mm length were cut from the raw polymer sample with a low speed saw. Subsequently the final size of the sample was adjusted by mechanical polishing in distilled water.

3.2 MEASUREMENTS

DMA test, loss tangent (damping or internal friction), $\tan(\phi)$, and dynamic shear modulus, G' , were measured as a function of the applied electrical field, E , in a mechanical spectrometer working in torsion at temperature of 318 K (± 0.25 K), in air [4]. The resonance frequency was around 1.5 Hz. Damping was determined by measuring the relative half

width of the squared resonance peak for a specimen driven into forced vibration using equation (14) [4]:

$$\tan(\phi) = \frac{\omega_2 - \omega_1}{\omega_0} \tag{14}$$

where ω_0 is the resonance frequency, and ω_1 and ω_2 are the frequencies at which the amplitude of oscillation has fallen to $1/\sqrt{2}$ of the maximum value. The errors of $\tan(\phi)$ and G' , being proportional to the squared oscillating frequency, are less than 1%. The maximum oscillating strain on the surface of the sample was 1×10^{-4} .

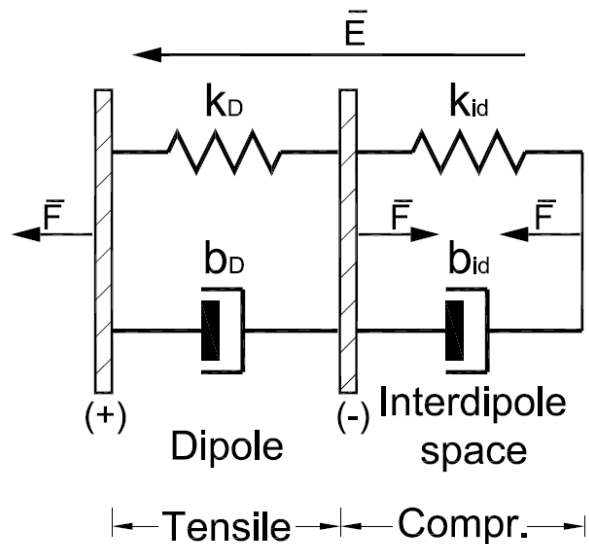


Figure 2. Elementary Unit Described Using the 2-parameter Voigt Model. Sub index D and id correspond to the dipole and inter-dipole element, respectively. F is the mechanical force. Taken from [7].

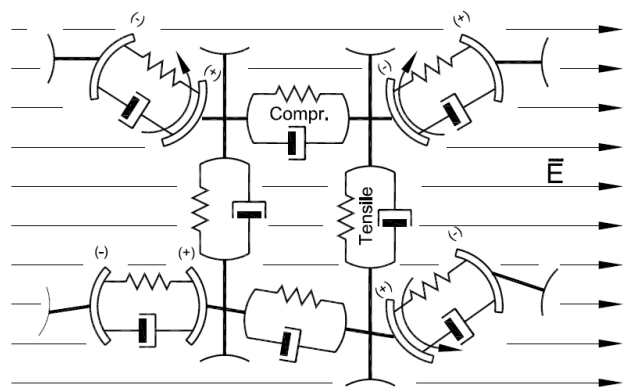


Figure 3. Two-dimensional Representation of a Solid Material Showing the Orientation Process due to the Application of the Electric Field. Taken from [7].

The electric field was produced by two electrodes placed at the sample position, lying in parallel direction to the torsion axis of the spectrometer, i.e. the resulting electric field is perpendicular to the torsion axis, Figure 4 [4]. Electrodes were connected to a variable DC high voltage power supply, giving rise to E values up to 1300 kV/m, at the sample location. The high voltage power supply was connected to a transformer

220/220 V, 5 A, to isolating the high voltage source from the line noise. In the shielded cable connected to the negative plate, a 9.1 M Ω (1%) resistance was inserted. The resistance was also under a grounded electromagnetic shield, see Figure 4. The voltage drop at the resistance due to the current changes in the power supply, caused by changes in the electrostriction of the oscillating dielectric sample material, was recorded by a digital storage high speed oscilloscope RIGOL 1052E. The oscilloscope is energized also by the transformer 220/220 V, 5 A. In order to improve the variation in the current the plates were placed with a gap of 1mm to the sample. It gives rise to an electric field at least twice higher than the one which was reported in [4]. The used electric field in the present work was 1300 kV/m.

4 THE MODEL. ELECTRO-RHEOLOGICAL DESCRIPTION OF DIELECTRIC MATERIALS EXHIBITING ELECTROSTRICTION

4.1 THE EXCITATION FROM AN ALTERNATING ELECTRIC FIELD

4.1.1 THE ONE DIMENSIONAL CASE

In this section the electrical response of a dielectric material with electrostriction subjected to an alternating electric field is studied. Regarding the flow diagram shown in Figure 1 here the sequence described by the line-dashed-arrows, is studied.

The dielectric material is described on the basis of an electro-rheological representation as shown in section 2.2. However, by considering a mean field approximation, the assembly of the dipole and inter-dipole elements for describing the dielectric material (Figure 2) will be averaged in the whole material through a unique Voigt unit, called hereafter equivalent dipole. Indeed, the whole material containing dipoles and inter-dipole spaces will be considered as a single dipole, see Figure 5.

In a solid subjected to an external electric field a strain by the electrostriction in the direction of the electric field is generated, which leads to a change in its volume that is,

$$V = V_0 \pm A x(t) \tag{15}$$

where A is the area of the electrically solicited zone, e.g. the area of the capacitor plate in Figure 5, and $x(t)$ is the displacement in the direction of the applied electric field. In fact, it is well known that electrostrictive effects in solids can lead to an increase or decrease in the volume, depending of the sign of the electrostriction [1-3, 9-11]. The case of an electrostrictive effect leading to the increase in volume will be developed in this paper. However, the case of an electrostrictive effect leading to a contraction of the solid implies only a change in the sign for the electrostrictive term, as it is easy to be inferred.

Differentiating equation (11), which equals the first term in equation (13), with respect to the time, we can obtain the instantaneous power related to the electrical field (see Figure 1) such that,

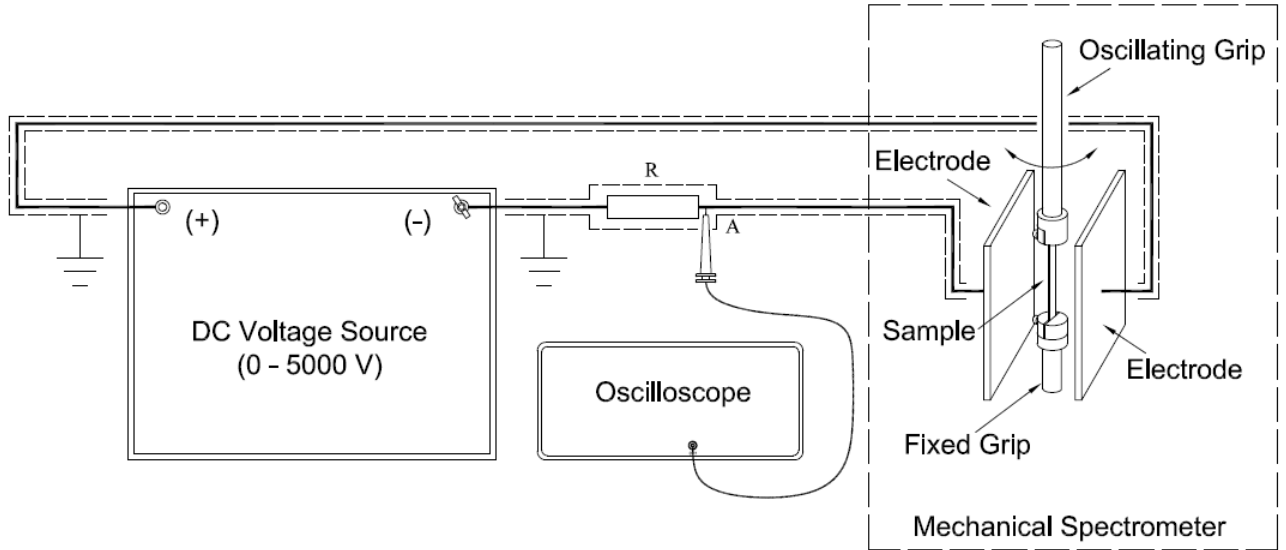


Figure 4. Experimental setup used for measuring electrostrictive effects from DMA tests conducted under high electric field. Zone inside the dashed line shows a schematic representation of the positioning of electrodes in the DMA equipment.

$$\frac{\partial W_a}{\partial t} = \varepsilon_o E(t) \frac{\partial E(t)}{\partial t} V(t) + \frac{1}{2} \varepsilon_o E(t)^2 \frac{\partial V(t)}{\partial t} \quad (16)$$

Then, relating equations (15) and (16) we obtain,

$$\begin{aligned} \frac{\partial W_a}{\partial t} = & \varepsilon_o E(t) \frac{\partial E(t)}{\partial t} V_o + \varepsilon_o E(t) \frac{\partial E(t)}{\partial t} A x(t) + \\ & + \frac{1}{2} \varepsilon_o E^2(t) A \frac{\partial x(t)}{\partial t} \end{aligned} \quad (17)$$

Adding the term of the transferred power related to the electro-rheological description for the equivalent dipole, Figure 5, we can write,

$$\begin{aligned} p_D = & \varepsilon_o E(t) \frac{\partial E(t)}{\partial t} V_o + F(t) \frac{\partial x(t)}{\partial t} + \\ & + \varepsilon_o E(t) \frac{\partial E(t)}{\partial t} A x(t) + \frac{1}{2} \varepsilon_o E(t)^2 A \frac{\partial x(t)}{\partial t} \end{aligned} \quad (18)$$

It should be stressed that equation (18) contains two more terms than the previously derived equation where the change in volume was neglected [7]. The new terms are related to the electrostrictive effect.

Taking the Laplace transform to the Voigt representation for the equivalent dipole in Figure 5 and anti-transforming it the displacement $x(t)$ in sustained oscillations takes the form [7],

$$x(t) = \frac{F}{k_{De}} \left[\frac{\sin(\omega \cdot t)}{(1 + (\omega \tau_{De})^2)} - \frac{(\omega \tau_{De})}{(1 + (\omega \tau_{De})^2)} \cos(\omega \cdot t) \right] \quad (19)$$

where $\omega = 2\pi f$, f being the frequency of the applied electric field and $\tau_{De} = b_{De}/k_{De}$ is the relaxation time corresponding to the Voigt representation [12, 13]. Besides, the corresponding displacement rate is given by,

$$\left. \frac{\partial x}{\partial t} \right|_{perm.} = \frac{F \omega}{k_{De}} \left[\frac{\omega \tau_{De}}{(1 + (\omega \tau_{De})^2)} \sin(\omega t) + \frac{\cos(\omega t)}{(1 + (\omega \tau_{De})^2)} \right] \quad (20)$$

By replacing equations (9), (19) and (20) in equation (18) and considering a sinusoidal behavior for the electric field, we can write,

$$\begin{aligned} p_D = & \varepsilon_o E^2 \cdot \omega \cdot \frac{\sin(2\omega t)}{2} \cdot V_o + \\ & + \frac{E^2 q_i^2 \omega}{4 k_{De}} \left[\frac{(\omega \tau_{De})}{(1 + (\omega \tau_{De})^2)} \sin^2(\omega t) + \right. \\ & \left. + \frac{1}{(1 + (\omega \tau_{De})^2)} \frac{\sin(2\omega t)}{2} \right] + \\ & + \frac{E^3 \varepsilon_o A q_i \omega}{4 k_{De}} \left[\frac{(\omega \tau_{De})}{(1 + (\omega \tau_{De})^2)} \sin^3(\omega t) + \right. \\ & \left. + \frac{1}{(1 + (\omega \tau_{De})^2)} \sin^2(\omega t) \cos(\omega t) \right] \end{aligned} \quad (21)$$

and working mathematically it results in

$$\begin{aligned} p_D = & U^2 \omega C_0 \left[\left(1 + \frac{q_i^2}{\varepsilon_o V 4 k_{De}} \cdot \frac{1}{1 + (\omega \tau_{De})^2} \right) \frac{\sin(2\omega t)}{2} + \right. \\ & \left. + \left(\frac{q_i^2}{\varepsilon_o V 4 k_{De}} \cdot \frac{(\omega \tau_{De})}{1 + (\omega \tau_{De})^2} \right) \sin^2 \omega t + \right. \end{aligned}$$

$$\begin{aligned}
 & + \left(\frac{U qi}{d^2 2 k_{De}} \cdot \frac{1}{1 + (\omega \tau_{De})^2} \right) \sin^2(\omega t) \cos(\omega t) - \\
 & - \left(\frac{U qi}{d^2 2 k_{De}} \cdot \frac{(\omega \tau_{De})}{1 + (\omega \tau_{De})^2} \right) \cos^2(\omega t) \sin(\omega t) + \\
 & + \left(\frac{U qi}{d^2 4 k_{De}} \cdot \frac{1}{1 + (\omega \tau_{De})^2} \right) \sin^2(\omega t) \cos(\omega t) + \\
 & + \left(\frac{U qi}{d^2 4 k_{De}} \cdot \frac{(\omega \tau_{De})}{1 + (\omega \tau_{De})^2} \right) \sin^3(\omega t) \quad (22)
 \end{aligned}$$

In fact, equation (22) represents the power transferred from the electric field to the whole dielectric material. Then, the electric current through the dielectric material calculated from equation (22) results in

$$i_D = U C_o \omega \left\{ \begin{aligned} & \left[1 + Q \frac{1}{(1 + (\omega \tau_{De})^2)} \right] \cos(\omega t) + \\ & + \left[Q \frac{(\omega \tau_{De})}{(1 + (\omega \tau_{De})^2)} \right] \sin(\omega t) + \\ & + 3EB \frac{1}{(1 + (\omega \tau_{De})^2)} \sin(2\omega t) - \\ & - 3EB \frac{(\omega \tau_{De})}{(1 + (\omega \tau_{De})^2)} \cos(2\omega t) - \\ & - EB \frac{(\omega \tau_{De})}{(1 + (\omega \tau_{De})^2)} \end{aligned} \right\} \quad (23)$$

Where $Q = \frac{q_i^2}{4 \epsilon_o V k_{De}}$ and $B = \frac{q_i}{8 d k_{De}}$

It should be emphasized that, the terms related to the harmonic contribution in equation (23) involve a dependence on the intensity of the electric field. Besides, it deserves of being mentioned that the second term, in equation (23), is related to the energy loss by irreversibility and not to the conductive current.

In the limit for low frequencies,

$$\frac{(\omega \tau_{De})}{(1 + (\omega \tau_{De})^2)} \rightarrow 0 \text{ and } \frac{1}{(1 + (\omega \tau_{De})^2)} \rightarrow 1 \quad (24)$$

equation (23) takes the form,

$$i_D = U C_o \omega \{ [1 + Q] \cos(\omega t) + 3EB \sin(2\omega t) \} \quad (25)$$

On the other side, for frequency values corresponding to the maximum of the relaxation peak

$$\frac{(\omega \tau_{De})}{(1 + (\omega \tau_{De})^2)} = \frac{1}{2} \text{ and } \frac{1}{(1 + (\omega \tau_{De})^2)} = \frac{1}{2} \quad (26)$$

equation (23) results in

$$\begin{aligned}
 i_D = U C_o \omega \left\{ \left[1 + \frac{Q}{2} \right] \cos(\omega t) + \frac{Q}{2} \sin(\omega t) + \right. \\
 \left. + \frac{3}{2} EB \sin(2\omega t) - \frac{3}{2} EB \cos(2\omega t) - \frac{1}{2} EB \right\} \quad (27)
 \end{aligned}$$

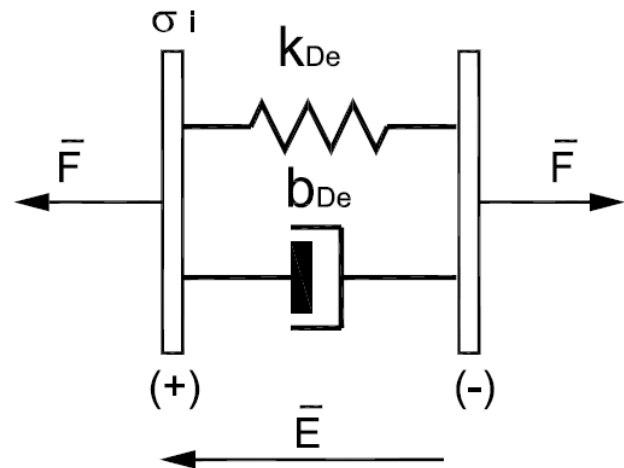


Figure 5. Equivalent dipole based on a Voigt unit. See explanation in the text.

The behavior of equation (27) as a function of time for an alternating electric field at 50 Hz is shown in Figure 6a. In addition, the response of equation (27) in the frequency domain is plotted in Figure 6b.

The prediction of this one-dimensional model regarding the appearance of harmonics in the capacitive current in dielectric materials subjected to an alternating electric field is in agreement with previous reported works [14-16]. For instance, the appearance of harmonics in the capacitive current of polymers excited by an alternating electric field has been reported in [15]. Moreover the compensation technique of the 2nd harmonic has been used widely for the molecular study of lipid membranes [16]. Indeed, a capacitor of variable gap between plates which are subjected to mechanical forces has been used to describe the lipid bilayer membranes [16-18]. Nevertheless, the elastic properties of a real lipid bilayer are inhomogeneous and the charges are really discrete. The bilayer elasticity is higher close to the polar groups than in the central area. The assumption of homogeneity both of the elasticity and the distribution of charges gave rise to discrepancies between experimental data and theoretical results [14, 16-19]. Regarding to our model here described, it is not targeted to the study of lipids membranes. However, as

the present model is developed in the frame of a mean field approximation its applicability to lipid membranes could be possible, after experimental check.

of stretching can be chosen in order to describe the volume change.

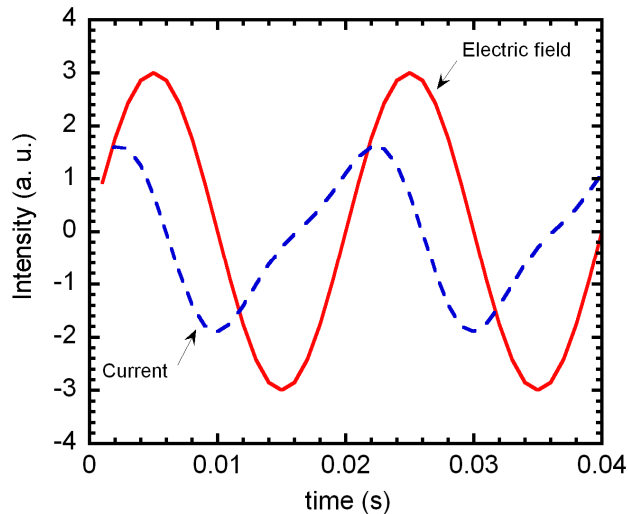


Figure 6a. Electric field (full line) and current from equation (27) (broken line) as a function of time.

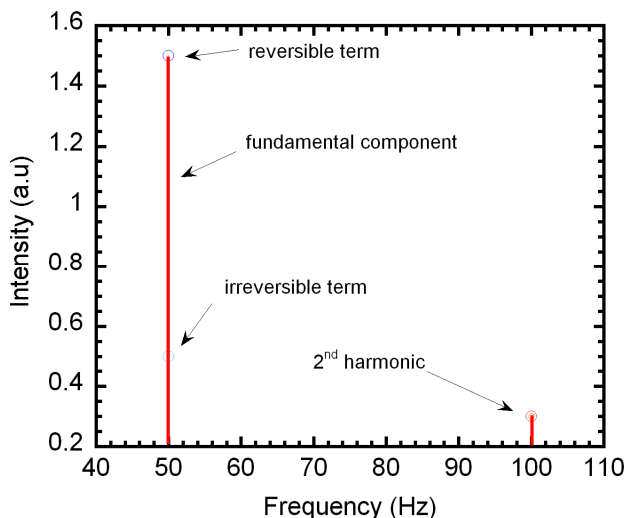


Figure 6b. Frequency spectra for the oscillating current from equation (27).

4.1.2 THE THREE DIMENSIONAL CASE

The arrangement of dipoles and inter-dipole elements shown in Figure 3 represents the two dimensional case. If a similar arrangements of dipoles is randomly located within a volume $V_o = l_x \cdot l_y \cdot l_z$, then, the volume of the dielectric material changes as a function of time, invoking changes in the three dimensional coordinate axis (x,y,z) . Then equation (15) transforms in

$$V(t) = V_o \pm \Delta V(t) = V_o \pm [\Delta V_x(t) + \Delta V_y(t) + \Delta V_z(t)] \quad (28)$$

The volume changes in each coordinate axis, $\Delta V_i(t)$ ($i=x,y,z$), can be deduced from Figure 7. The initial, undistorted volume, $V_o = l_x \cdot l_y \cdot l_z$, suffers stretching sequentially in each axis x , y and z , labeled as $x(t)$, $y(t)$ and $z(t)$; respectively. This procedure is not unique and other sequences

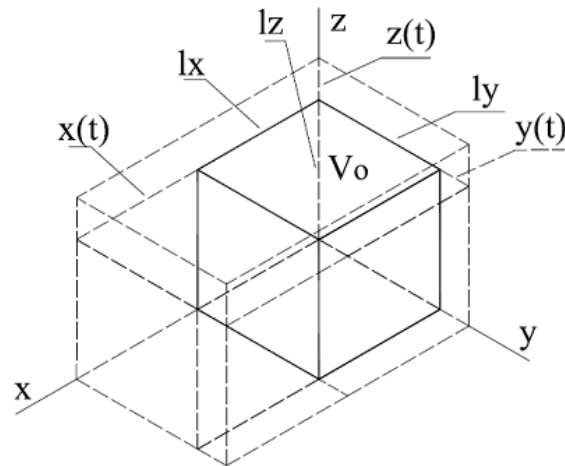


Figure 7. Initial volume $V_o = l_x \cdot l_y \cdot l_z$ containing the random distribution of dipoles (full lines). Dashed lines indicate the volume increase promoted by the application of an electric field.

Then each $\Delta V_i(t)$ can be written as

$$\Delta V_x(t) = l_y \cdot l_z \cdot x(t) \quad (29)$$

$$\Delta V_y(t) = [l_x + x(t)] \cdot y(t) \cdot l_z \quad (30)$$

$$\Delta V_z(t) = [l_x + x(t)] \cdot [l_y + y(t)] \cdot z(t) \quad (31)$$

In the analysis developed below, the direction x will be chosen as the direction where the electric field is applied, so, we will reduce the stretching $y(t)$ and $z(t)$ (see Figure 7) as a function of stretching $x(t)$ through appropriate constants C_y and C_z in such a way that

$$y(t) = C_y \cdot x(t) \quad (32)$$

$$z(t) = C_z \cdot x(t) \quad (33)$$

C_y and C_z are proportionality constants related to the reorganization of dipoles which exhibit some misalignment with the direction of the field. Indeed, the electric field promotes both a rotation and a stretching of the dipoles randomly embedded into V_o , giving rise to an mean contribution for strain on the x -direction. By replacing equations (29) to (33) in equation (28) and working mathematically we can obtain

$$V(t) = V_o + A x(t) + B x(t)^2 + C x(t)^3 \quad (34)$$

wherein

$$A = l_y \cdot l_z \pm C_y \cdot l_x \cdot l_z \pm l_x \cdot l_y \cdot C_z \quad (35)$$

$$B = C_y \cdot l_z \pm l_y \cdot C_z \pm l_x \cdot C_y \cdot C_z \quad (36)$$

$$C = \pm C_y, C_z \quad (37)$$

As it was described for the one-dimensional case, Section 4.1.1, the instantaneous power related to the electric field is given by equation (16). Then, by replacing in the terms $\partial V(t)/\partial t$ in equation (16), the derivative of equation (28) with respect to the time and by considering an alternating electric field in the form $E(t) = E \sin(\omega t)$, it results in

$$\begin{aligned} \frac{\partial W_a}{\partial t} = & \varepsilon_o \omega E^2 \sin(\omega t) \cos(\omega t) \left[\frac{V_o + Ax(t) + Bx(t)^2 + Cx(t)^3}{+Bx(t)^2 + Cx(t)^3} \right] + \\ & + \frac{1}{2} \varepsilon_o E^2 \sin^2(\omega t) \left[\frac{A \frac{\partial x(t)}{\partial t} + 2Bx(t) \frac{\partial x(t)}{\partial t} + 3Cx(t)^2 \frac{\partial x(t)}{\partial t}}{\frac{\partial x(t)}{\partial t}} \right] \quad (38) \end{aligned}$$

Let's now study the transferred power towards the rheological structure of the dielectric material. As it was shown in previous Sections, the transferred power to the rheological components equals [7]

$$\frac{\partial W_m}{\partial t} = F_x(t) \frac{\partial x(t)}{\partial t} \quad (39)$$

wherein $F_x(t)$ is the average force on the x-direction, which gives rise to the displacement $x(t)$.

Similarly to the reduction of variables made above for writing the volume, equations (17) to (22), let us assume that energies for y- and z- directions could be reduced to the energy in the x-direction through appropriate D_y and D_z constants, such that

$$\frac{\partial W_m}{\partial t} = F_x(t) \frac{\partial x(t)}{\partial t} + D_y F_x(t) \frac{\partial x(t)}{\partial t} + D_z F_x(t) \frac{\partial x(t)}{\partial t} \quad (40)$$

$$\frac{\partial W_m}{\partial t} = F_x(t) \frac{\partial x(t)}{\partial t} [1 + D_y + D_z] \quad (41)$$

By defining $D = 1 + D_y + D_z$, equation (41) results

$$\frac{\partial W_m}{\partial t} = D F_x(t) \frac{\partial x(t)}{\partial t} \quad (42)$$

It is convenient to be mentioned here that all constants C_i , (equations 32 and 33) and D_i (equation 41), $i = y, z$; were defined in order to represent the electrostrictive contribution on the three coordinate axes; reduced to the x-axis. Indeed, it allows the mathematical handling of a quasi one-dimensional case, which involves the contribution from the other directions, instead of the heavy mathematical treatment of the formal three-dimensional case.

Following a straightforward analysis according to the one-dimensional case, the whole dielectric material will be averaged through a mean field approximation as an equivalent dipole, Figure 5.

Considering the mechanical force, promoted by the electric field, as a function of time in the x-direction with the form

$$F_x(t) = F_x \sin(\omega t) \quad (43)$$

$$\text{with } F_x = \frac{1}{2} q_i E \quad (44)$$

and replacing equations (43) and (44) in equation(42), the transferred total power, $p = \partial W_T / \partial t$, equals

$$\begin{aligned} p = \frac{\partial W_T}{\partial t} = & \frac{\partial W_m}{\partial t} + \frac{\partial W_a}{\partial t} = D \frac{1}{2} q_i E \sin(\omega t) \frac{\partial x(t)}{\partial t} + \\ & + V_o \varepsilon_o \omega E^2 \sin(\omega t) \cos(\omega t) + A \varepsilon_o \omega E^2 \\ & \sin(\omega t) \cos(\omega t) x(t) + B \varepsilon_o \omega E^2 \sin(\omega t) \\ & \cos(\omega t) x(t)^2 + C \varepsilon_o \omega E^2 \sin(\omega t) \cos(\omega t) x(t)^3 + \\ & + A \frac{1}{2} \varepsilon_o E^2 \sin^2(\omega t) \frac{\partial x(t)}{\partial t} + 2B \frac{1}{2} \varepsilon_o E^2 \sin^2(\omega t) \\ & x(t) \frac{\partial x(t)}{\partial t} + 3C \frac{1}{2} \varepsilon_o E^2 \sin^2(\omega t) x(t)^2 \frac{\partial x(t)}{\partial t} \quad (45) \end{aligned}$$

As it has been solved earlier in [7], the displacement promoted by the electric dipole in sustained oscillations in the x- direction can be written as

$$x(t) = \frac{1}{2} q_i E \frac{1}{k_{De}} \left[\frac{\sin(\omega \tau_{De})}{(1 + (\omega \tau_{De})^2)} - \frac{(\omega \tau_{De})}{(1 + (\omega \tau_{De})^2)} \cos(\omega t) \right] \quad (46)$$

Consequently, its displacement rate results

$$\frac{\partial x}{\partial t} = \frac{1}{2} q_i E \frac{\omega}{k_{De}} \left[\frac{\omega \tau_{De}}{(1 + (\omega \tau_{De})^2)} \sin(\omega t) + \frac{\cos(\omega t)}{(1 + (\omega \tau_{De})^2)} \right] \quad (47)$$

By replacing equations (46) and (47) in equation (45), and working mathematically, the total power transferred to the dielectric material can be described by

$$\begin{aligned} p = & V_o \varepsilon_o \omega E^2 \sin(\omega t) \{ \cos(\omega t) + Q \sin(\omega t) \\ & \frac{\omega \tau_{De}}{(1 + (\omega \tau_{De})^2)} + Q \cos(\omega t) \frac{1}{(1 + (\omega \tau_{De})^2)} + Q_A \sin(\omega t) \\ & \cos(\omega t) \frac{1}{(1 + (\omega \tau_{De})^2)} - Q_A \cos^2(\omega t) \frac{(\omega \tau_{De})}{(1 + (\omega \tau_{De})^2)} + \end{aligned}$$

$$\begin{aligned}
 & + \frac{1}{2} Q_A \sin^2(\omega t) \frac{\omega \tau_{De}}{(1+(\omega \tau_{De})^2)} + \frac{1}{2} Q_A \sin(\omega t) \cos(\omega t) \\
 & \frac{1}{(1+(\omega \tau_{De})^2)} + Q_B \sin^2(\omega t) \cos(\omega t) \frac{1}{(1+(\omega \tau_{De})^2)^2} - \\
 & - Q_B \sin(\omega t) \cos^2(\omega t) \frac{(\omega \tau_{De})}{(1+(\omega \tau_{De})^2)^2} + Q_B \cos^3(\omega t) \\
 & \frac{(\omega \tau_{De})^2}{(1+(\omega \tau_{De})^2)^2} + Q_B \sin^3(\omega t) \frac{\omega \tau_{De}}{(1+(\omega \tau_{De})^2)^2} + Q_B \sin^2(\omega t) \\
 & \cos(\omega t) \frac{1}{(1+(\omega \tau_{De})^2)^2} - Q_B \sin^2(\omega t) \cos(\omega t) \frac{(\omega \tau_{De})^2}{(1+(\omega \tau_{De})^2)^2} - \\
 & - Q_B \sin(\omega t) \cos^2(\omega t) \frac{(\omega \tau_{De})}{(1+(\omega \tau_{De})^2)^2} + Q_C \cos(\omega t) \\
 & \sin^3(\omega t) \frac{1}{(1+(\omega \tau_{De})^2)^3} - 3 Q_C \sin^2(\omega t) \cos^2(\omega t) \\
 & \frac{(\omega \tau_{De})}{(1+(\omega \tau_{De})^2)^3} + 3 Q_C \sin(\omega t) \cos^3(\omega t) \frac{(\omega \tau_{De})^2}{(1+(\omega \tau_{De})^2)^3} - \\
 & - Q_C \cos^4(\omega t) \frac{(\omega \tau_{De})^3}{(1+(\omega \tau_{De})^2)^3} + \frac{3}{2} Q_C \sin^4(\omega t) \frac{\omega \tau_{De}}{(1+(\omega \tau_{De})^2)^3} - \\
 & - 3 Q_C \sin^3(\omega t) \cos(\omega t) \frac{(\omega \tau_{De})^2}{(1+(\omega \tau_{De})^2)^3} + \frac{3}{2} Q_C \sin^2(\omega t) \\
 & \cos^2(\omega t) \frac{(\omega \tau_{De})^3}{(1+(\omega \tau_{De})^2)^3} + \frac{3}{2} Q_C \sin^3(\omega t) \cos(\omega t) \frac{1}{(1+(\omega \tau_{De})^2)^3} - \\
 & - 3 Q_C \sin^2(\omega t) \cos^2(\omega t) \frac{(\omega \tau_{De})}{(1+(\omega \tau_{De})^2)^3} + \frac{3}{2} Q_C \sin(\omega t) \\
 & \left. \cos^3(\omega t) \frac{(\omega \tau_{De})^2}{(1+(\omega \tau_{De})^2)^3} \right\} \quad (48)
 \end{aligned}$$

wherein

$$Q = \frac{q_i^2 D}{4 \varepsilon_o V_o k_{De}} \quad (49)$$

$$Q_A = \frac{q_i A E}{2 V_o k_{De}} \quad Q_A = \frac{A}{V_o} \left(\frac{q_i E}{2 k_{De}} \right) \quad (50)$$

$$Q_B = \frac{q_i^2 B E^2}{4 V_o k_{De}^2} \quad Q_B = \frac{B}{V_o} \left(\frac{q_i E}{2 k_{De}} \right)^2 \quad (51)$$

$$Q_C = \frac{q_i^3 C E^3}{8 V_o k_{De}^3} \quad Q_C = \frac{C}{V_o} \left(\frac{q_i E}{2 k_{De}} \right)^3 \quad (52)$$

In the limit of low frequencies, the following conditions are satisfied

$$\frac{(\omega \tau_{De})^n}{(1+(\omega \tau_{De})^2)^m} \rightarrow 0 \quad \text{and} \quad \frac{1}{(1+(\omega \tau_{De})^2)^m} \rightarrow 1 \quad (53)$$

where m and n are integers ≥ 1 . In addition, by using trigonometric relationships for $\sin(2\omega t)$, $\cos(2\omega t)$, $\sin(3\omega t)$, $\cos(3\omega t)$, $\sin(4\omega t)$ and $\cos(4\omega t)$ [20], then equation (48) simplifies to

$$\begin{aligned}
 p = V_o \varepsilon_o \omega E^2 \sin(\omega t) \{ [1+Q] \cos(\omega t) + \\
 + \frac{3}{4} Q_A \sin(2\omega t) - \frac{2}{3} Q_B \cos(3\omega t) - \frac{5}{8} Q_C \sin(4\omega t) \\
 + R(\omega t) \} \quad (54)
 \end{aligned}$$

with

$$R(\omega t) = \frac{2}{3} Q_B \cos^3(\omega t) + \frac{5}{2} Q_C \sin(\omega t) \cos^3(\omega t) \quad (55)$$

Taking in consideration an alternating voltage in the form, $U(t) = U \sin(\omega t)$, equation (54) can be written as

$$\begin{aligned}
 p = A_o d \varepsilon_o \omega \left(\frac{U}{d} \right)^2 \sin(\omega t) \{ [1+Q] \cos(\omega t) + \\
 + \frac{3}{4} Q_A \sin(2\omega t) - \frac{2}{3} Q_B \cos(3\omega t) - \frac{3}{8} Q_C \sin(4\omega t) + \\
 + R(\omega t) \} \quad (56)
 \end{aligned}$$

wherein d is the gap between the plates of the effective dipole (Figure 5) at potential $U(t)$, caused by the electric field $E(t)$.

So, the electric current, $i(t)$, through the dielectric material equals

$$\begin{aligned}
 i(t) = \omega C_o U \{ [1+Q] \cos(\omega t) + \\
 + \frac{3}{4} Q_A \sin(2\omega t) - \frac{2}{3} Q_B \cos(3\omega t) - \\
 - \frac{5}{8} Q_C \sin(4\omega t) + R(\omega t) \} \quad (57)
 \end{aligned}$$

with $C_o = \varepsilon_o A_o/d$. As it can be inferred from equation (57), the volume change promoted by electrostriction gives rise to harmonics terms.

For frequency values corresponding to the maximum of the relaxation peak, the conditions gave in equations (26) are satisfied, then the current obtained from equation (57) results

$$i = \omega C_o U \left\{ \begin{array}{l} \frac{Q}{2} \sin(\omega t) + \left[1 + \frac{Q}{2} \right] \cos(\omega t) + \\ + \frac{3Q_A}{8} \sin(2\omega t) - \frac{Q_A}{2} \cos(2\omega t) - \\ - \frac{Q_B}{4} \sin(3\omega t) + \frac{Q_B}{4} \cos(3\omega t) + \\ + \frac{Q_C}{64} \sin(4\omega t) + \frac{Q_C}{16} \cos(4\omega t) + R(\omega t) \end{array} \right\} \quad (58)$$

where $R(\omega, t)$ includes again the terms with some power in \sin or \cos , that is

$$\begin{aligned} R(\omega, t) = & \frac{Q_B}{4} \sin(\omega t) \cos^2(\omega t) + Q_B \sin^2(\omega t) \cos(\omega t) - \\ & - \frac{Q_A}{4} \sin^2(\omega t) + \frac{Q_C}{2} \sin(\omega t) \cos^3(\omega t) - \\ & - 3 \frac{Q_C}{16} \sin^2(\omega t) \cos^2(\omega t) - 3 \frac{Q_C}{16} \cos^4(\omega t) + \\ & + 2 \frac{Q_C}{16} \sin^4(\omega t) \end{aligned} \quad (59)$$

The behavior of equation (58) as a function of time for an alternating electric field at 50 Hz is shown in Figure 8a. In addition, the response in frequency domain of equation (58) is plotted in Figure 8b. As it can be seen either from equation (58) and Figure 8, higher harmonics are predicted by the new model when the change in volume is taken into consideration. These results are also in agreement with previously reported works [14-16]. Therefore, the coupling of more electrostrictive effects lying in different sollicitation directions, give rise to the development of higher harmonics in the capacitive current when the material is subjected to an alternating electric field.

4.2 THE EXCITATION FROM AN OSCILLATING MECHANICAL FIELD

In this section, the electrical response of a dielectric electrostrictive material subjected to an oscillating mechanical force, $F(t)$, in combination with a constant electric field, E , (electromechanical coupling) will be studied. In fact, as is indicated by the alt-dashed arrows in Figure 1, it can be strongly suggested that the electrical response $i(t)$ involves the contribution of both the electrical and mechanical fields. Thus the present study will be focused only on the one-dimensional case. This consideration does not diminish the results of the present Section, due to the three-dimensional case study is targeted to the appearance of more harmonics in the electrical current, as it was already shown.

The whole dielectric material is considered again as an effective dipole based on a Voigt unit, as shown in Figure 5. Figure 9 shows the non-perturbed (upper) and the sollicited

(lower) states, respectively. The perturbed state due to the superposition of the constant electric and the oscillatory mechanical fields, corresponds to the maximum stretching of the equivalent dipole.

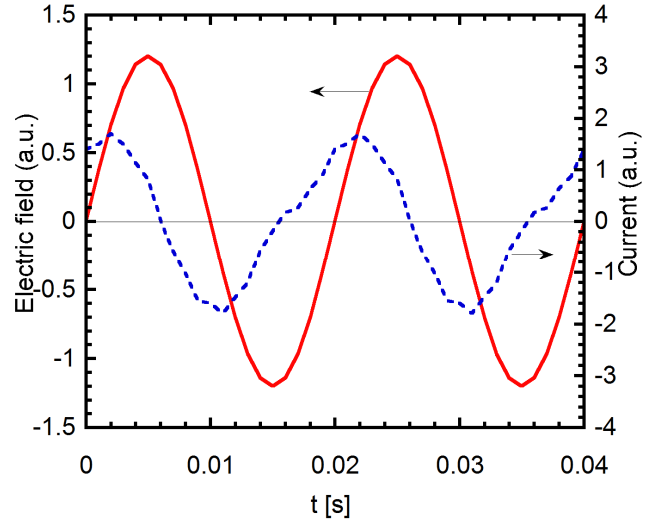


Figure 8a. Electric field (full line) and current from equation (58) (broken line) as a function of time.

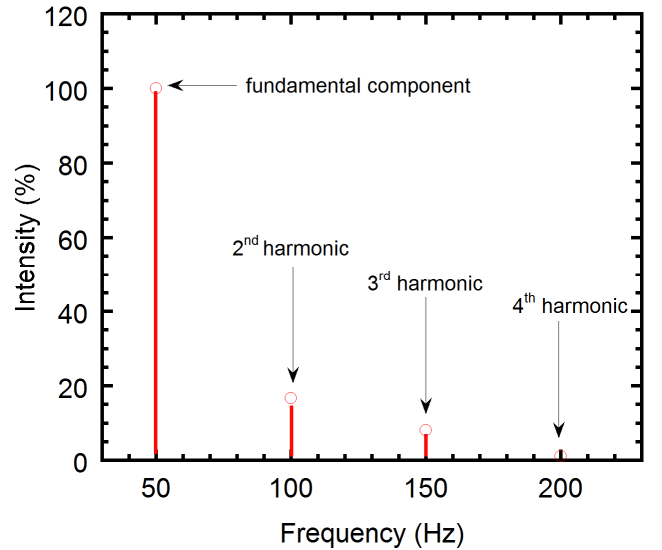


Figure 8b. Frequency spectra for the oscillating current from equation (58).

Considering a dielectric material subjected both to a constant electric field, E , and to a mechanical excitation in the form $F(t) = F \sin(\omega t)$, the instant power transferred to the electro-rheological coupling results,

$$\frac{\partial W_a}{\partial t} = \frac{1}{2} \varepsilon_o E^2 \frac{\partial V(t)}{\partial t} \quad (60)$$

In contrast to the case developed in the previous section, the energy provided from the mechanical system, W_m , is transferred to the electrical system through the electro-

rheological coupling. In fact, the electrical system only receives the contribution from the electromechanical coupling, i.e. W_a . Therefore, the oscillatory mechanical field generates a current through the dielectric material of the same frequency. The expression for W_a in the present case, takes the form

$$i(t) = \frac{E \epsilon_o \epsilon A \omega}{2} \left[\frac{(\omega \tau_{De})}{(1 + (\omega \tau_{De})^2)} \sin(\omega t) + \frac{\cos(\omega t)}{(1 + (\omega \tau_{De})^2)} \right] \quad (64)$$

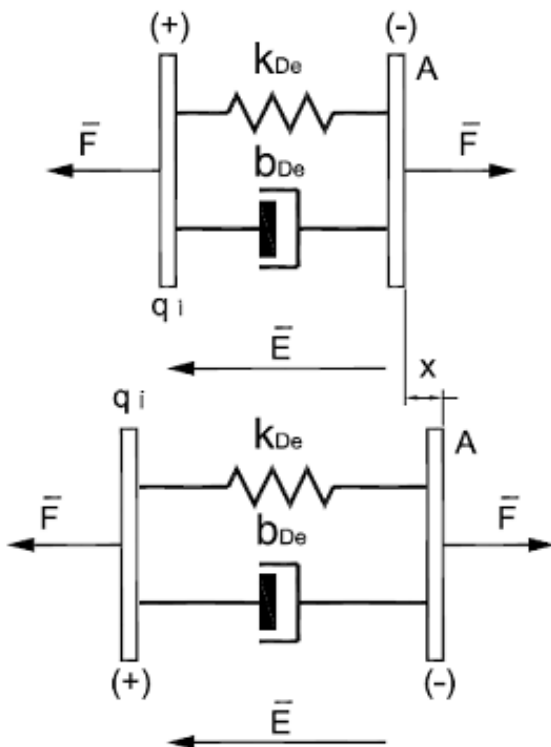


Figure 9. Equivalent dipole based on a Voigt unit. Upper plot: undistorted state. Lower plot: distorted material after the application of the electric and mechanical fields.

$$W_a = \frac{1}{2} \epsilon_o E^2 V(t) \quad (61)$$

wherein the electric field is independent on time in the present case. In addition, the volume change due to a mechanical excitation is given by the equation (15). Taking the derivative of equation (61) with respect to the time we can write

$$\frac{\partial W_a}{\partial t} = \frac{1}{2} \epsilon_o E^2 A \frac{\partial x(t)}{\partial t} \quad (62)$$

Using the displacement rate of the dielectric material as an effective dipole based in a Voigt unit given by equation (20), the expression for the instant power equals

$$p_D = \frac{E^2 \epsilon_o F A \omega}{2 k_{De}} \left[\frac{(\omega \tau_{De})}{(1 + (\omega \tau_{De})^2)} \sin(\omega t) + \frac{\cos(\omega t)}{(1 + (\omega \tau_{De})^2)} \right] \quad (63)$$

Consequently, after mathematical work, the current takes the form

It should be emphasized that the resulting current through the dielectric is proportional to the intensity of the electric field and also to the mechanical strain. In fact, equation (64) clearly reveals the electrostriction effect, since a current appears in the dielectric as a consequence of the oscillatory mechanical field.

5 COMPARISON OF MODEL RESULTS WITH EXPERIMENTAL DATA FROM DMA TESTS CONDUCTED UNDER HIGH ELECTRICAL FIELD.

The experimental verification of the capability of describing the electrostriction phenomenon from the electro-rheological representation shown in the present work was made through DMA tests conducted under high electric field on polyamide and polyethylene samples. DMA test involves an oscillating stress as a probe [21], so by superposing a direct electric field, the theoretical results from Section 4.2 can be verified. Indeed, from Section 4.2, it is proposed that an alternating current appears in the dielectric material as a consequence of the oscillating force due to the electrostrictive effect.

Figure 10 shows the behavior of damping and dynamic modulus as a function of the applied electric field for the PA sample. As it can be seen from the Figure, damping (circles) decreases and dynamic modulus (triangles) increases as the strength in the electric field increases. After reaching the maximum value of electric field strength the field strength was again reduced. Damping and modulus measurement values in both cases, increasing and decreasing field strength, were identical within the measurement error. That means, no hysteretic effect was found.

In contrast, damping and modulus measurement values of PE samples do not show any dependence on the strength of the electric field. Thus, damping and modulus behavior is not a function of the applied electric field, E . The damping and modulus values measured at nil electric field for PE and PA are shown in Table 1.

Table 1. $\tan(\phi)$ and G' measured at nil electric field in PE and PA (at Room Temperature).

	PE	PA
$\tan(\phi)$	0.10	0.11
G' (MPa)	70	250

The behavior for PA as a function of the field strength is in agreement with previously reported data on styrene butadiene rubber which were explained by means of the inclusion model for dielectric materials [4-6]. In fact, the applied electric field

promotes the stretching and/or rotation of electric dipoles which increase the internal stresses of the matrix. It leads to a decrease in the chains mobility of the polymer, giving rise to the decrease and increase of damping and modulus, respectively.

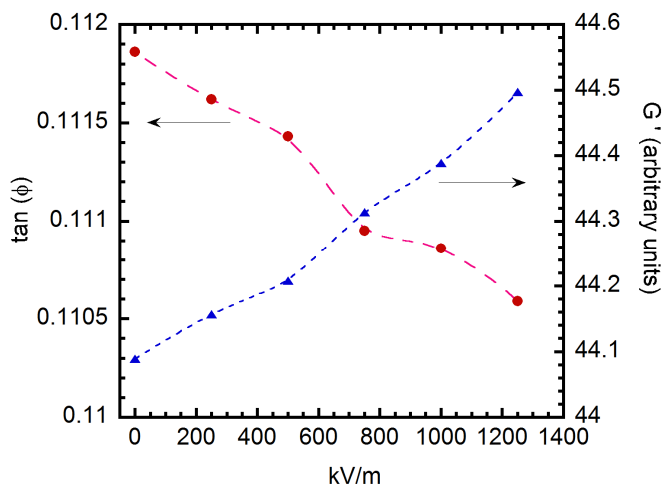


Figure 10. $\tan(\Phi)$ (circles) and G' (triangles) as a function of the electric field strength for a PA sample.

As it can be seen from Figure 4, the experimental setup is slightly different from the one reported in [4]. The negative electrode is in series with the resistance R (see Figure 4). R measures the voltage drop due to the oscillating current promoted by the electrostrictive effect. Electrical work must be done by the power supply in order to compensate the modification of the polarization vector, due to the change in the dipoles arrangement, promoted by the oscillating stress due to the electrostrictive effect.

In order to assess that the alternating current is promoted only by changes in the polarization state of the sample, a PE sample with equal size and shape as the PA sample was measured. Moreover, the maximum oscillating strain was also identical for both PA and PE samples. No alternate current in PE samples was detected. Therefore, some contribution from the slight twist of sample between the plates can be neglected. Consequently, a contribution to the current promoted by a change in capacity, due to the modification in the geometrical arrangement of the sample at the spectrometer, can be neglected.

The alternating current recorded by the oscilloscope at the A point, see Figure 4, and the oscillating strain, during DMA measurements performed under 1300 kV/m are shown in Figure 11. The recorded voltage from R was in the order of some mV.

The alternating current and oscillating strain were subsequently mathematically handled by means of Fourier transform [22]. In order to obtain the phase difference between the mechanical oscillation, $\varepsilon(t)$, and the current, $i(t)$ (equation 64), and also avoid the electrical noise; the complex coefficients of the Fourier discrete series of $\varepsilon(t)$, and $i(t)$ were calculated, see Appendix for details. Figure 12 shows the

behavior of the mechanical oscillation and the alternating current measured at point A after the Fourier transform. Both signals were recorded by a high speed oscilloscope (see Section 3.2) simultaneously, so the mismatch in time for both recorded waves is completely negligible.

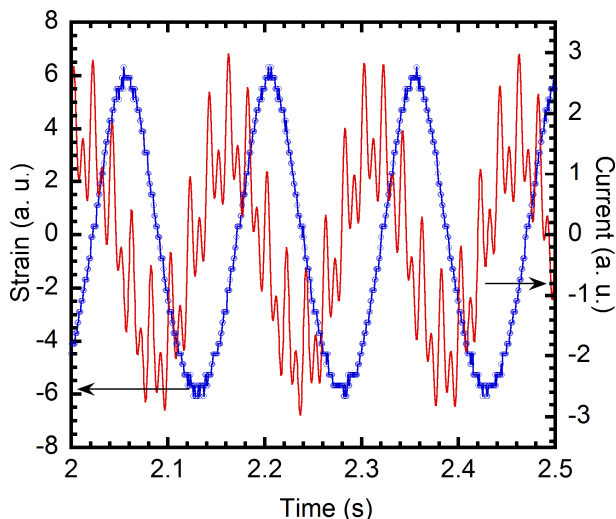


Figure 11. Current promoted from the electrostriction phenomenon due to the oscillating mechanical field and oscillating strain, for PA sample.

As it can be seen from the Figure, the current curve overtakes the strain one in a slightly higher value than $\pi/2$, which is in a good agreement with the theoretical predictions of the model developed in Section 4.2. The obtained shift from the Fourier analysis between the strain and current is $95^\circ / 0.528 \pi$, which emphasizes that the rheological contribution of the measured current is promoted by the electrostrictive coupling from the oscillating strain. Indeed, equation (64) predicts an overtakes of around $\pi/2$ far of the maximum of the relaxation peak. Taking in consideration that for PA at 318 K there is not reported dielectric relaxation processes [11, 23], a shift of around $\pi/2$ between the strain and current is reasonable. Moreover, in a dynamic mechanical analysis test for a given material, the strain lags to the stress by a ϕ angle. Thus, considering a damping of 0.11 (see Table 1), it leads to a lag angle close to five degrees. So, as in Figure 12 we are plotting strain instead stress; the overtake of current regarding strain in 5 degrees higher is in very good agreement.

6 SUMMARY

An electro-rheological model, based on a Voigt equivalent dipole which involves the electrostriction phenomenon, was developed. The model was based on a mean field approximation as an averaging of the mechanical and electrical properties.

The response of the model was studied considering both, electrical and mechanical excitations. The one- and three-dimensional cases were studied.

In the case of an alternating electrical excitation the model reveals the appearance of harmonics in the current through the dielectric material promoted by the electrostriction

phenomenon. The one-dimensional case can resolve the appearance of the second harmonic, while the three-dimensional case resolves the appearance of higher harmonics. In contrast, for the case of an oscillating mechanical excitation, the model predicts a current which overtakes the driving mechanical oscillation. Moreover, in this last case an excellent correlation between the model and experimental results was obtained from dynamic mechanical analysis tests conducted under high electric field.

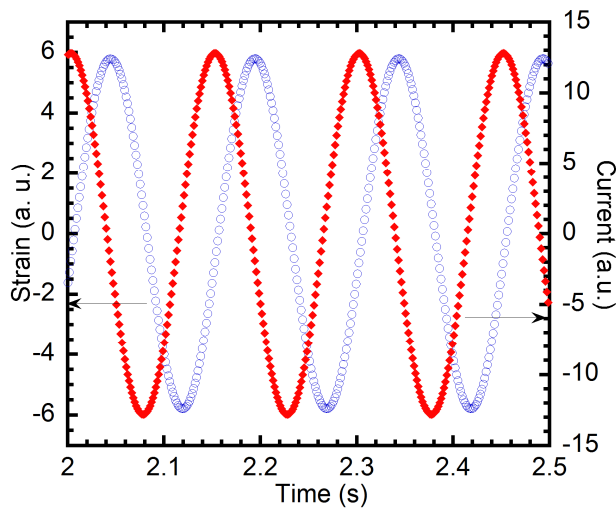


Figure 12. Current promoted from the electrostriction phenomenon due to the oscillating mechanical field after Fourier transform, for PA sample. Empty symbols: Strain. Full symbols: Current.

APPENDIX

In order to calculate the phase difference between the mechanical oscillation, $\varepsilon(t)$, and the current, $I_C(t)$, and also to avoid the electrical noise, we get the complex coefficients of the Fourier discrete series of the mechanical and electrical waves. For this purpose, we use the well known expression,

$$c_k = \frac{1}{N} \sum_{n=1}^N X[n] e^{-jk\Omega n} \quad (65)$$

where $X[n]$ is the vector containing the values of the wave for points equally spaced in time, N the total number of points in a period and $\Omega = 2\pi/N$. The Fourier discrete series is,

$$s(t) = \sum_{n=1}^N c_k e^{jk\Omega t} \quad (66)$$

Due to the random nature of the electrical noise, we use 31 periods instead of one to calculate the complex coefficients, c_k . Thus, the 31st harmonic corresponds to the fundamental frequency, which is the one of our interest. From the spectra obtained for each wave, the modulus of the complex coefficients corresponding to the homonymous harmonics, the 31st harmonics are used.

In this way, the signals of the mechanical and the electrical oscillations (without electrical noise) result,

$$\varepsilon(t) = \varepsilon_{31} \cos(\omega_{31,mec} t - \theta_{31,mec}) \quad (67)$$

$$I_C(t) = I_{C_{31}} \cos(\omega_{31,elec} t - \theta_{31,elec}) \quad (68)$$

Equations (67) and (68) were used for the plotted curves in Figure 11. In addition, the shift between both waves is obtained from

$$\phi_{31} = \theta_{31,mec} - \theta_{31,elec} = \text{tg}^{-1} \left(\frac{b_{31,mec}}{a_{31,mec}} \right) - \text{tg}^{-1} \left(\frac{b_{31,elec}}{a_{31,elec}} \right) \quad (69)$$

where a and b are the binomial coefficients of the Fourier series related to the cosine and sine, respectively; such that $a = 2 \text{Re}(c_k)$ and $b = -2 \text{Im}(c_k)$

ACKNOWLEDGMENT

This work was partially supported by the CONICET-PIP No. 179CO and 2098, the PID-UNR ING 450 and ING 453 (2014-2017) and the Collaboration Agreement between the Clausthal University of Technology and the Universidad Nacional de Rosario, Res. 2292/2015.

REFERENCES

- [1] L. D. Landau and E. M. Lifshitz, *Classical Theory of the Fields*, Vol. 2, Reverté: Barcelona, Spain, 1973.
- [2] K. J. Pascoe, *Properties of Materials for Electrical Engineers*, Wiley, New York, USA, 1973
- [3] J. D. Jackson, *Classical Electrodynamics*; Alhambra: Madrid, Spain, 1980.
- [4] O. A. Lambri, R. R. Mocellini, F. Tarditti, F. G. Bonifacich, D. Gargicevich, G. I. Zelada, C. E. Boschetti, "Internal Stresses in the Electrostriction Phenomenon Viewed Through Dynamic Mechanical Analysis Studies Conducted under Electric Field", *IEEE Trans. Dielectr. Electr. Insul.*, Vol. 21, No. 5, pp. 2070–2080, 2014.
- [5] R. R. Mocellini, O. A. Lambri, C. L. Matteo, J. A. García, G. I. Zelada-Lambri, P. A. Sorichetti, F. Plazaola, A. Rodríguez-Garrara, and F. A. Sánchez, "Elastic misfit in two-phase polymer", *Polymer*, Vol. 50, pp. 4696 – 4705, 2009.
- [6] O. A. Lambri, F. Plazaola, E. Axpe, R. R. Mocellini, G. I. Zelada-Lambri, J. A. García, C. L. Matteo, and P. A. Sorichetti, "Modification of the mesoscopic structure in neutron irradiated EPDM viewed through positron annihilation spectroscopy and dynamic mechanical analysis", *Nuclear Inst. Meth. B*, pp. 269, 336 – 344, 2011.
- [7] R. R. Mocellini, G. I. Zelada-Lambri, O. A. Lambri, C. L. Matteo, P. A. Sorichetti, "Electro-rheological description of liquid and solid dielectrics applied to two-phase polymers: a study of EPDM", *IEEE Trans. Dielectr. Electr. Insul.*, Vol. 13, No. 6, pp. 1358 – 1370, 2006.
- [8] R.R. Mocellini, O. A. Lambri, C. L. Matteo, P. A. Sorichetti, "Dielectric Properties and Viscoelastic Response in Two-Phase Polymers", *IEEE Trans. Dielectr. Electr. Insul.*, Vol. 15, No. 4, pp. 982 – 993, 2008.
- [9] F. C. Brown, *The Physics of Solids*, W. A. Benjamin, INC, New York, USA, 1967.
- [10] A. R. Von Hippel, *Dielectrics and Waves*, Wiley: New York, USA, 1954.
- [11] J. P. Runt and J. J. Fitzgerald, *Dielectric Spectroscopy of Polymeric Materials, Fundamentals and Applications*, American Chemical Society, Washington D.C., USA, 1997.
- [12] B. J. Lazan, *Damping of Materials and Members in Structural Mechanics*, Pergamon, London, UK, 1968.

- [13] N. W. Tschoegl, *The Phenomenological Theory of Linear Viscoelastic Behaviour*, Springer Verlag, Berlin, Germany, 1989.
- [14] W. Carius, "Voltage dependence of bilayer membrane capacitance. Harmonic response to AC excitation with DC bias", *J. Colloid Inter. Sci.*, Vol. 57, pp. 301-307, 1976.
- [15] J. A. Malecki, "Phenomenological Model of Nonlinear Dielectric Losses Related to the Intrinsic Conductivity of Dielectrics", *Europ. Phys. J. B*, Vol. 39, pp.235-240, 2004.
- [16] V. I. Passechnik, "Estimates of the intramembrane field through the harmonics of capacitive current in inhomogeneous bilayer lipid membranes", *Bioelectrochemistry*, Vol. 54, pp. 67-73, 2001.
- [17] V. I. Passechnik, V. S. Sokolov, "Estimation of electrochrome dyes position in the bilayer through the 2nd harmonic of capacitive current", *Bioelectrochemistry*, Vol. 55, pp. 47-51, 2002.
- [18] T. Heimburg, "The Capacitance and Electromechanical Coupling of Lipid Membranes Close to Transitions: The Effect of Electrostriction", *Biophysical Journal*, Vol. 103, pp. 918-929, 2012.
- [19] J. Kilian, S. Kalinowski, J. Kochana, P. Knihnicki, "A new capacitive sensor based on electrostriction phenomenon. Application for determination of ionic surfactants", *Procedia Eng.*, Vol. 47, pp. 1338-1341, 2012.
- [20] M. Abramowitz and I. A. Stegun, *Handbook of mathematical functions*, National Bureau of Standards, Washington D.C., USA, 1964.
- [21] R. Schaller, G. Fantozzi and G. Gremaud, Eds., *Mechanical Spectroscopy*, Trans Tech Publications Ltd., Switzerland, 2001.
- [22] W. H. Press, S. A. Teukolsky, W. T. Vetterling and B. P. Flannery, *Numerical Recipes in FORTRAN 77, The Art of Scientific Computing*, 2nd Edition, Cambridge University Press, UK, 1992.
- [23] P. A. M. Steeman, F. H. J. Maurer, "Dielectric properties of polyamide-4,6", *Polymer*, Vol. 33, pp. 4236-4241, 1992.



Ricardo Raúl Mocellini, was born in San Lorenzo, Argentina in 1956. He got his degree as Electrical Engineer and the Ph.D. degree from Rosario National University (UNR) in 2006 and 2014, respectively. Nowadays he is a scientist at the Laboratory of Materials (LEIM), EIE, FCEIA, UNR. He is focused on the study of dielectric properties of technological materials. Eng. Mocellini is also an associate professor at EIE, FCEIA, UNR. He is also working at the Projects and Electrical Maintenance Department of PETROBRAS ENERGIA Plant in Puerto General San Martín, since 1992.



Osvaldo Agustín Lambri was born in Rosario, Argentina in 1963. He obtained the B.Sc. and M.Sc. (physics, 1989) degrees from the Rosario National University (UNR) and the Ph.D. degree in physics (1993), focused on materials science) from the same University. Post-doctoral position at the Laboratory of Materials in the University of the Basque Country, Bilbao, Spain. Guest Scientists at the Institut für Werkstoffkunde und Werkstofftechnik, Clausthal University of Technology, Clausthal Zellerfeld, Germany and at the Faculty of Science and Technology of the University of the Basque Country, Basque Country, Spain. Dr. Lambri is a member of the National Council of Research Staff of Argentina (CONICET). Since 2002 he is head of the Laboratory of Materials (LEIM) at the Electrical Engineering School (EIE) of the Faculty of Science and Engineering (FCEIA) of the UNR – CONICET and an Associate Professor of Electrical Materials at EIE, FCEIA, UNR. Nowadays he is also head of the Center of Technology and Research in Electrical Engineering, FCEIA, UNR. He also was leader of Research Projects at the Institute Laue Langevin, Grenoble, France. His current research areas include the mechanical properties and phase transitions of super-alloys and refractory metals and the mechanical and electrical properties of polymers and dielectric materials.



Federico Guillermo Bonifacich was born in Rosario, Argentina in 1989. He got his degree as Electrical Engineer from Rosario National University (UNR) in 2012. Nowadays he has got a fellowship from the National Council of Research of Argentina (CONICET). He also has a Doctoral position at the Laboratory of

Materials (LEIM-CONICET) at the Electrical Engineering School (EIE) of the Faculty of Science and Engineering (FCEIA) of the UNR. He is focused on the study of ferromagnetic shape memory alloys and their applications in superelastic devices, sensors and actuators.



UNR.

Damián Gargicevich was born in Casilda, Argentina in 1989. He got his degree as Electrical Engineer from Rosario National University (UNR) in 2012. Nowadays he has got a fellowship from the National Council of Research of Argentina (CONICET). He also has a Doctoral position at the Laboratory of Materials (LEIM-CONICET) at the Electrical Engineering School (EIE) of the Faculty of Science and Engineering (FCEIA) of the



UNR. He is focused on the study of the relation of mechanical and electrical properties of polymer materials used in Electrical Industry.

Federico Tarditti was born in Rosario, Argentina in 1988. He got his degree as Electrical Engineer from Rosario National University (UNR) in 2012. Nowadays he has got a fellowship from the National Council of Research of Argentina (CONICET). He also has a Doctoral position at the Laboratory of Materials (LEIM-CONICET) at the Electrical Engineering School (EIE) of the Faculty of Science and Engineering (FCEIA) of the



1994 until 1999 he worked in automotive industry. There he was responsible for research and development of materials for automotive applications. In 1999 he returned to Clausthal University of Technology in the Department of Materials Sciences where he finished his habilitation in Materials Science in 2007. Now he is the head of the department of Materials Science. His current research interests include Internal Friction, magnetic properties of soft magnetic metallic materials and soft magnetic composites, and thermal as well as electrical properties of composite materials. In these areas he published about seventy scientific papers in peer reviewed journals.

Bernd Weidenfeller was born in Germany in 1961. He received his diploma degree in physics from the University of Münster, Germany, in 1988. Before he received his Ph.D. degree in materials science and engineering in 1994 at Clausthal University of Technology in Clausthal-Zellerfeld, Germany, he developed from 1988 until 1992 a photoemission electron microscope at the Institute of Physics in Clausthal.



2012 he is working in automotive industry.

Mathias Anhalt was born in Germany in 1977. He received his diploma degree in materials science from the Clausthal University of Technology in 2004. From 2005 to 2012 he was scientist at the Faculty of Natural Science of the same university. His main research areas are magnetic, thermal and electrical properties and dynamic mechanical behaviour of particle filled polymers. Since



engineering and is a professor at that institute since 2000. His research interests are internal friction and soft magnetic materials. In these areas he is a knowledgeable advisor for leading manufacturer of electromagnetic balances. He published about two-hundred scientific papers in peer reviewed journals.

Werner Riehemann was born in Germany in 1952. He received is Diploma degree in physics in 1978 and his Ph.D. degree in metal physics at the Institute for Metals Research in 1983, both from the University of Münster, Germany. Since 1984 he is scientist at the Institute of Materials Science and Engineering at Clausthal University of Technology, in Clausthal-Zellerfeld, Germany. There he prepared his habilitation in materials science and